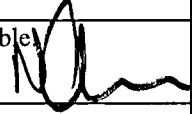NGU Report 99.052

Palaeoproterozoic magnesite-stromatolite-
dolomite-'red beds' association, Russian Karelia:
palaeoenvironmental constraints on the 2.0 Ga
positive carbon isotope shift.

NGU

Norges geologiske undersøkelse
Geological Survey of Norway

Geological Survey of Norway
N-7441 Trondheim, Norway
Tel.: 47 73 90 40 11
Telefax 47 73 92 16 20

REPORT

Report no.: 99.052	ISSN 0800-3416	Grading: Open

Authors: Melezhik, V.A., Fallick, A.E., Medvedev, P.V., Makarikhin, V.V.	Client: INTAS-RFBR, Brussels-Moscow

County: Russia, Norway, Scotland	Commune:

Map-sheet name (M=1:250.000)	Map-sheet no. and -name (M=1:50.000)

Deposit name and grid-reference:	Number of pages: 39 Price (NOK): 113 Map enclosures:

Fieldwork carried out: 1998	Date of report: 15.11.99	Project no.: 2741.00/95-928	Person responsible: N. Cook

Summary:

The ca. 2000 Ma Tulomozerskaya Formation, Russian Karelia, represents the most ^{13}C-rich carbonates (up to +18‰) which have ever been reported. The implication of this excursion for our understanding of the coeval global geodynamic carbon cycle is not clear, but the interpretation of the maximum δ^{13}C is crucially dependent on the palaeoenvironmental setting of the sediments, also on the interplay between global and local forcing functions of isotope fractionation. The formation is composed of a 800 m-thick magnesite-stromatolite-dolomite-'red beds' succession. Terrigeneous red beds developed throughout the sequence exhibit great variation in thickness and lithofacies. They represent a meandering fluvial system over a carbonate coastal plain, periodically flooded supratidal zone, ponded tidal flat and playa lake environments under high-temperature, evaporitic conditions. A significant component of the carbonate rocks is stromatolitic, formed in peritidal, low-energy, protected bights or barred basins. The red, flat-laminated, stromatolitic dolostones of Members A and C are assigned to evaporative ephemeral ponds, coastal sabkhas and playa lakes. A small portion of Member B, D and G carbonates may represent deposits accumulated in relatively 'open' marine environments. An explosion of stromatolite-forming microbial communities along with restricted, evaporitic, shallow-water environments are the local factors which might have caused isotopic disequilibrium between atmospheric CO_2 and dissolved inorganic carbon in local reservoirs. This should be taken into account when interpreting carbon isotopic data and attempting to discriminate between the local enrichment in ^{13}C and the background of globally enhanced δ^{13}C values.

Keywords: Palaeoproterozoic	Dolomite	Magnesite
Stromatolite	Red beds	Evaporites
Carbonate platform	Playa	Sabkha

CONTENTS

FIGURES

3

TABLES

1.   INTRODUCTION

Since the pioneering work of Schidlowski et al. (1976), the existence of unusually ^{13}C-enriched carbonates in Africa deposited at around 2.3 Ga (the Lomagundi event) has puzzled geologists. While this so-called Lomagundi event was ascribed to locally enhanced burial of organic matter in a restricted basin (Schidlowski et al. 1976), two additional discoveries of ca. 2.0 Ga-old carbonates with extremely positive δ^{13}C values led to a reassessment of this event as global in nature (Baker & Fallick 1989a, b). The carbon isotope excursion was interpreted as the result of an increase of the carbon fraction buried as organic matter globally.

However, despite the fact that the global significance of the Palaeoproterozoic high δ^{13}C values has recently been re-emphasised (Karhu & Holland 1996), the geological data necessary for understanding the mechanism responsible for the δ^{13}C values as high as +10 to +18‰ are not yet available (Melezhik & Fallick 1996). The local carbonate δ^{13}C may consist of a global background value together with a regional signature dependent on the specific palaeoenvironmental setting; therefore, the true global background value of δ^{13}C for this period of time remains a subject for debate (Melezhik & Fallick 1997), and our understanding of the carbon cycle is incomplete.

To date, most reported high δ^{13}C values for Palaeoproterozoic successions are based on material that has very limited information on depositional environments (e.g., Schidlowski et al. 1976; Karhu 1993; Baker & Fallick 1989a, b; Melezhik & Fallick 1996). Consequently, discrimination between global and local factors contributing to this excursion has not yet been made. In order to cover some gaps in our knowledge related to the Palaeoproterozoic δ^{13}C excursion, an international project entitled 'World-wide 2 billion-year-old isotopically heavy carbonate carbon: the evolutionary significance and driving forces' was set up. The two year-long project is supported by INTAS-RFBR (Brussels-Moscow) and aims to contribute new data on one of the most challenging problems in Palaeoproterozoic Earth history. In this report we present some of the results obtained by the international research group working in the framework of this project.

The focus of this work is a succession of magnesite-stromatolite-dolomite-'red beds' represented by the ca. 2 billion-year-old Tulomozerskay Formation in the Onega Lake area, Russian Karelia (Fig. 1). Ever since Yudovich et al. (1991) published $\delta^{13}C$ values up to 18‰, the Tulomozerskay carbonates have been the most ^{13}C enriched primary sedimentary carbonates ever reported, thus occupying an exceptional position in the Palaeoproterozoic high-$\delta^{13}C$ records and calling for a detailed assessment of the palaeoenvironment. The formation was intensively drilled for the purpose of establishing and describing the Palaeoproterozoic stratotype of the Russian Federation. Consequently, drillcore material has become available enabling detailed sedimentological and palaeontological study.

This report addresses the depositional environments of the Tulomozerskay carbonate succession in order to assist in the interpretation of ^{13}C-rich carbonates, and consequently our understanding of the carbon cycle in the Palaeoproterozoic.

2.   GEOLOGICAL BACKGROUND

The Palaeoproterozoic Tulomozerskaya succession is preserved in a synform exposed on the northern side of Lake Onega, as well as on its islands and peninsulas, occupying an area of 10,000 km^2 (Fig. 1). The Onega synform consists of a number of smaller NW-SE trending and SE-plunging synforms and antiforms. The sequence of the N. Onega Lake area includes seven formations (Fig. 2), namely, the Pal'ozerskaya, Jangozerskaya, Medvezhegorskaya, Tulomozerskaya, Zaonezhskaya, Suisarskaya and Vashezerskaya formations (Sokolov 1987). The Palaeoproterozoic rocks, with the Pal'ozerskaya basal polymict conglomerates and diamictites, unconformably overlie the Archaean substratum. The Jangozerskaya, Medvezhegorskaya and Tulomozerskaya formations are collectively known as the Jatulian Group (Sederholm 1899; Eskola 1919; Väyrynen 1933; Kratz 1963; Sokolov 1970, 1980; Negrutza 1984). The stratotype section of the Jatulian Group has been described in detail by
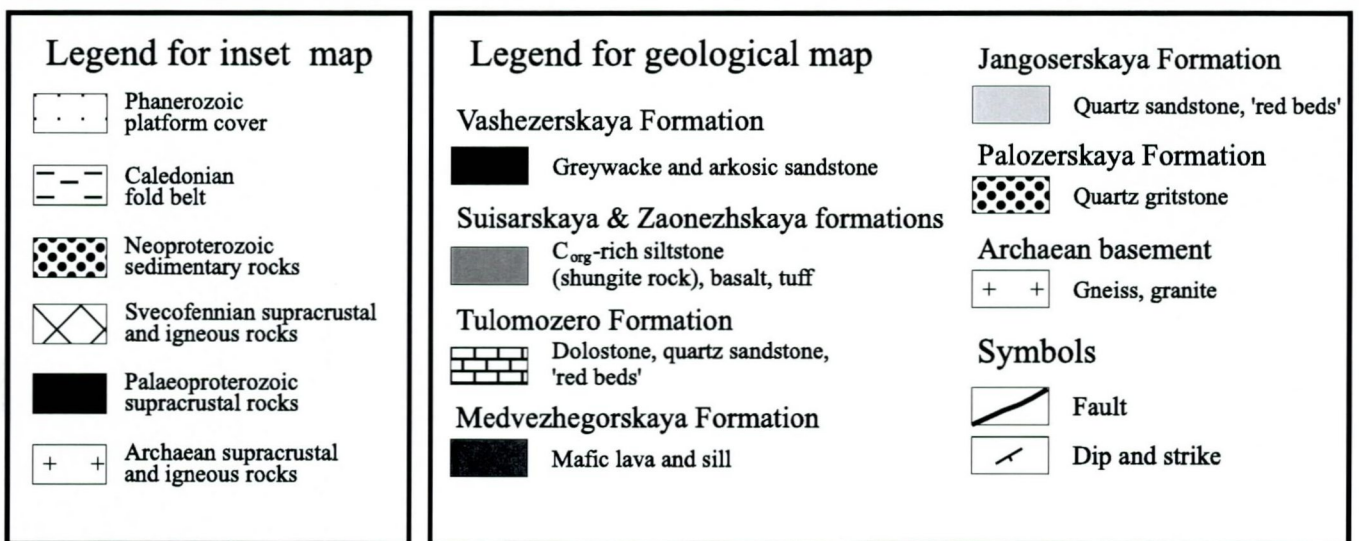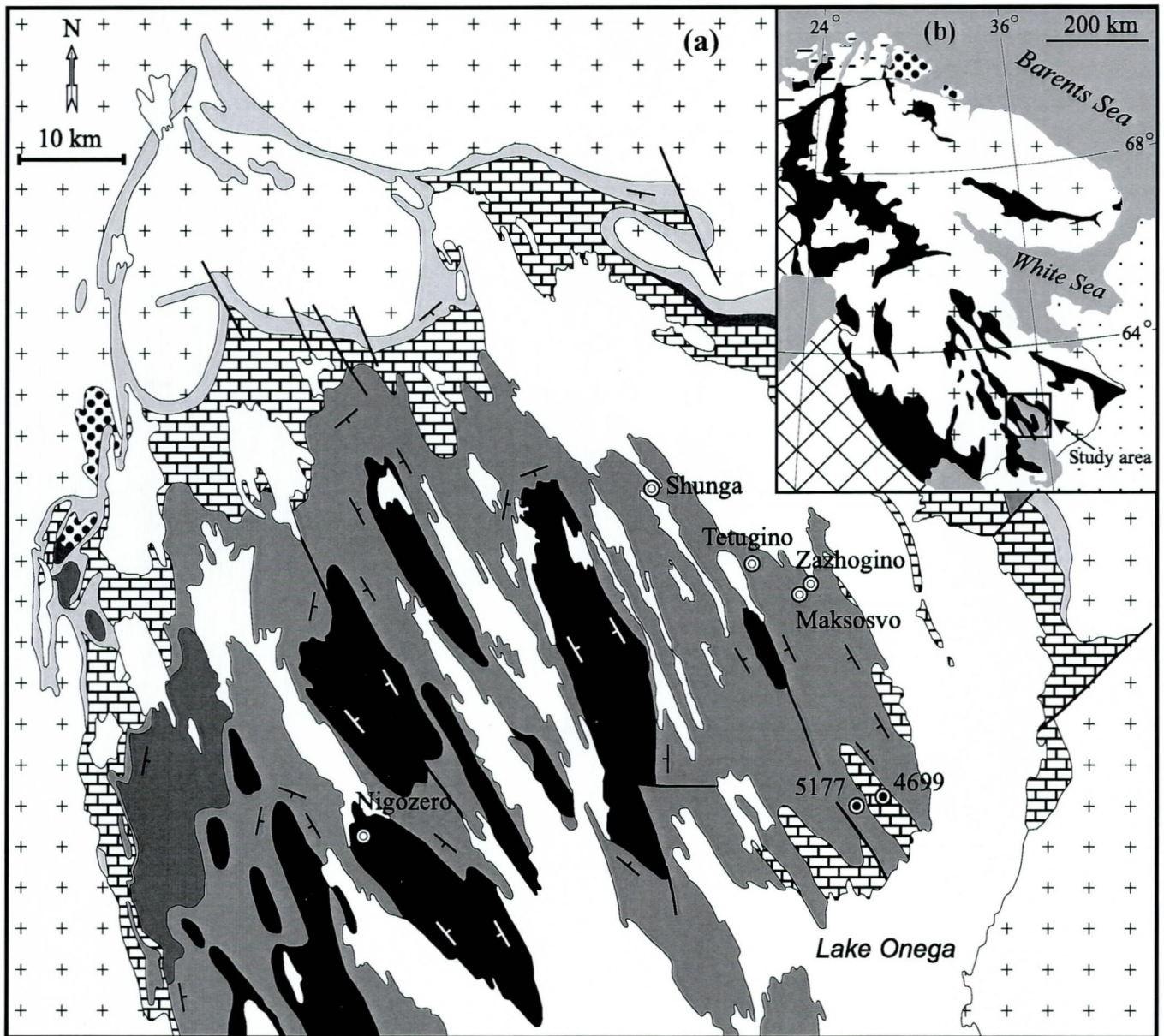
Figure 1. *(a) Geographical and geological location of the study area (marked by square), and (b) geological map of the northern Onega Lake area (simplified from Akhmedov et al., 1993).*

The map contains the following labels and legend:

(a) map with features:
- Shunga
- Tetugino
- Zazhogino
- Maksosvo
- Nigozero
- 5177   4699
- Lake Onega
- N
- 10 km
- 200 km

(b) inset map:
- 24°, 36°
- Barents Sea
- White Sea
- 68°, 64°
- Study area

Legend for inset map
- Phanerozoic platform cover
- Caledonian fold belt
- Neoproterozoic sedimentary rocks
- Svecofennian supracrustal and igneous rocks
- Palaeoproterozoic supracrustal rocks
- Archaean supracrustal and igneous rocks

Legend for geological map

Vashezerskaya Formation
- Greywacke and arkosic sandstone

Suisarskaya & Zaonezhskaya formations
- C_{org}-rich siltstone (shungite rock), basalt, tuff

Tulomozero Formation
- Dolostone, quartz sandstone, 'red beds'

Medvezhegorskaya Formation
- Mafic lava and sill

Jangoserskaya Formation
- Quartz sandstone, 'red beds'

Palozerskaya Formation
- Quartz gritstone

Archaean basement
- Gneiss, granite

Symbols
- Fault
- Dip and strike

7

Figure 1 content:

LITHOSTRATIGRAPHIC UNIT		THICKNESS	DRILL HOLE POSITION
Vepsi	Shokshinskaya	1000	
Vepsi	Petrozavodskaya	450	
Kalevi (Livvi)	Kondopozhskaya & Vashezerskaya	700	
Ludikovi	Suisarskaya	400	
Ludikovi	Zaonezhskaya	1500	5177 800.7 m / 4699 806 m
Jatuli	Tulomozerskaya	800	
Jatuli	Medvezhegorskaya	70	
Jatuli	Jangozerskaya	50	
Sarioli	Pal'ozerskaya	400	
Sumi	Kumsinskaya	300	

1	2		3
	zn_1		
'Red Bed'-Dolomite Member	H	20*	Layers with *Calevia ruokanesis*
Oncolite-Dolomite Member	G	30	
	F	25	Layers with *Butinella*
Dolomite-Mudstone Member	E	110	
Hematite-Sandstone Member	E	110	
Pisolith-Dolomite Member	D	60	Layers with *Omachtenia kintsiensis*
Siltstone Member	C	105	
Stromatolite-Dolomite Member	B	90	Layers with *Sundosia*
Magnesite-Dolomite Member	B	90	Layers with *Nuclephyton*
Phosphate-Dolomite Member			
Limestone-Dolomite-Mudstone Member	A	250	Layers with *Lukanoa*

Figure 1. *Stratigraphic position of the studied drillholes (left column) and lithostratigraphical subdivisions (right column) of the northern Onega Lake area as suggested by: 1 - Akhmedov et al. (1993), 2 - present authors, 3 - Makarikhin and Medvedev (cited in Akhmedov et al. 1993). The thickness in the right column is shown in metres as measured in drillhole 4699 (Member A) and 5177 (Members B, C, D, E, F, G and H). zn_1 is the Zaonezhskaya Formation.*

Russian geologists in the Onega Lake area, Russian Karelia. In the stratotype area (e.g. Sokolov 1987) the Jatulian succession begins with the 50-120 m-thick Jangozersakaya Formation, which rests either conformably on the Sariolian conglomerates or unconformably on weathered Archaean gneisses and granites. The Jangozersakaya strata comprise predominantly oxidised, red terrigenous sediments characterised by cross-bedding and desiccation cracks and subordinate calcareous siltstones. These rocks are conformably overlain by the 70 m-thick Medvezhegorskaya Formation. This formation consists of mafic lava with subordinate cross-bedded quartz sandstones, gritstones and 'red beds'. The Tulomozerskaya Formation conformably overlies the Medvezhegorskaya succession. The formation is described in detail in the following sections.

The three Jatulian formations are unconformably overlain by organic carbon-rich siltstones and mudstones (shungite rocks[*]) with subordinate dolostones of the 1,500 m-thick Zaonezhskaya Formation. This is followed by the Suisarskaya Formation, a 400 m-thick succession of basalts intercalated with numerous gabbro sills. A gabbro intrusion from the upper part of the Suisarskaya Formation has given a Sm-Nd mineral isochron age of 1980±27 Ma (Pukhtel' et al. 1992). The succession ends with the 190 m-thick Vashezerskaya Formation comprising greywacke and arkosic sandstones.

The Palaeoproterozoic rocks were deformed and underwent greenschist facies metamorphism during the 1.8 Ga Svekofennian orogeny. The paragenesis chlorite-actinolite-epidote reflects a temperature of 300-350°C.

3.   LITHOSTRATIGRAPHICAL SUBDIVISION OF THE
       TULOMOZERSKAYA FORMATION

Carbonate samples analysed in this study were obtained from drillcores in the Tulomozerskaya Formation. The drillholes 5177 (35°25′00″E, 62°14′29″N) and 4699 (35°28′00″E, 62°14′30″N) were made by the Karelian Geological Expedition and intersect

---

[*] Shungite is a mineral comprising nanocrystalline, free carbon. The mineral was discovered a 100 years ago in Karelia, near the village of Shunga from which its name originates. Later, all rocks (chert, dolostone, limestone, siltstone, tuff) containing the mineral shungite have been termed by Russians as 'shungite rocks'.

an 800 m-thick succession (Fig. 2) located in the southeastern part of the Onega palaeobasin (Fig. 1).

Based on the lithology and mineralogical composition, the Tulomozerskaya Formation has been divided into a number of 'piles' (Akhmedov et al. 1993), renamed here as 'members' (Fig. 2) in accordance with the International Stratigraphic Code (ISSC, 1976). For practical reasons and for consistency we have substituted letters for Russian names, starting with 'A' for the lowermost Limestone-Dolomite-Mudstone Member. The whole succession, consisting of the eight lithostratigraphic members (A-H), can also be divided into six biostratigraphic units each with distinctive stromatolites, oncolites and microfossils (Fig. 2). Principal feature of the lithostratigraphic Members A to H are characterised in Table 1.

4.   LITHOFACIES OF THE TULOMOZERSKAYA FORMATION

Facies analysis is based on drillcore material supported by available outcrops in the area adjacent to the drilling site, which provide good information on structural features and their spatial distribution. The main lithofacies recognised in the sequence are described below.

Lithofacies I consists of reddish-grey to grey, fine- to medium-grained, either ripple-marked and cross-stratified or structureless, quartz sandstones with dolomite cement. Dolomite-bearing quartz sandstones occur as 8 to 10 m-thick beds in the lower part of Members A and B (Fig. 3, 4) where they have an erosional base. Tabular sets of cross-stratification 1 to 3 cm thick are common structural developments of Member A and B sandstones. The sandstone beds of Member A occasionally bear small-scale channels filled with cross-bedded, coarse-grained sandstones. Rare asymmetric ripples have low relief with amplitudes of 0.3 to 0.5 cm and wavelengths of 1-4 cm. The lithological observations suggest that the dolomite-bearing quartz sandstones represent a meandering fluvial system over a lower energy, carbonate coastal plain.

Table 1. *Table 1. Interpreted depositional environments of the Tulomozerskaya Formation.*

Member	Thickness, m	Litho-facies	Rock assemblage	Colour	Stromatolite morphology	Interpreted depositional environment
H	20	VII, X	Finely laminated dolostone and dolomitic marl	Red	Spaced, low-relief bioherms, flat-laminated stomatolites.	Upper tidal zone of carbonate flat (VII, X).
G	30	X	Dolostone	Pink, brown	Very closely spaced bioherms, oncolites.	Intertidal setting fully exposed to wave action (X).
F	25	III, V	Siltstone, sandstone, dolostone, amygdaloidal basalt		Flat-laminated stromatolites, oncolites.	Playa lake, ponded tidal flat (III); protected bight and lagoon (V); tidal carbonate flat, drained depressions and ephemeral ponds (X).
E	110	III, V, X	Quartz sandstone, siltstone with a carbonate matrix; two-three intervals of dolostone	Pink	Flat-laminated stromatolites.	Playa lake, ponded tidal flat (III); upper tidal zone, protected bight or lagoon (V); playa lake (X).
D	60	IV, V, VIII, IX, X	Dolostone with magnesite layers, dolostone collapse breccia, siltstone	Grey, pink	Oncolites; spaced, single, large columns; laterally continuous biostromes.	Tidal and supratidal sandflat (IV); upper tidal zone, protected bight and lagoon (V); playa lake, sabkha (VIII, IX); intertidal setting fully exposed to wave action (X).

Table 1. *(continued).*

| Mem-ber	Thick-ness, m	Litho-facies	Rock assemblage	Colour	Stromatolite morphology	Interpreted depositional environment
C	105	IV, V, VIII, X	Finely laminated siltstone and sandstone intercalated with dolostone	Red	Laterally continuous biostromes; flat-laminated stromatolites; oncolites.	Tidal and supratidal sandflat (IV); upper tidal zone of protected bight or lagoon (V); playa lake, sabkha (VIII); upper tidal carbonate flat, drained depressions and ephemeral ponds (X).
B	90	I, VI, IX, X	Dolostone with 1 to 2 m thick magnesite band, quartz sandstone	Pale grey	Laterally continuous biostromes; spaced bioherms; spaced, single, large columns; oncolites; flat-laminated stromatolites.	Meandering fluvial system over a carbonate, coastal plain (I); protected bight (VI); playa lake, sabkha (IX); bight both protected and fully exposed to wave action; upper tidal carbonate flat, ephemeral ponds (X).
A	250	I, II, IV, V, VIII, IX, X	Dolostone alternating with quartz sandstone and finely laminated siltstone	Pink	Flat-laminated stromatolites; markedly divergent, small, columnar stromatolites.	Meandering fluvial system over a coastal plain (I); periodically flooded tidal flat (II); lower-energy tidal and supratidal sandflat (IV); upper tidal protected bight and lagoon (V); playa lake, sabkha (VIII, IX); upper tidal of carbonate flat, ephemeral ponds (X).
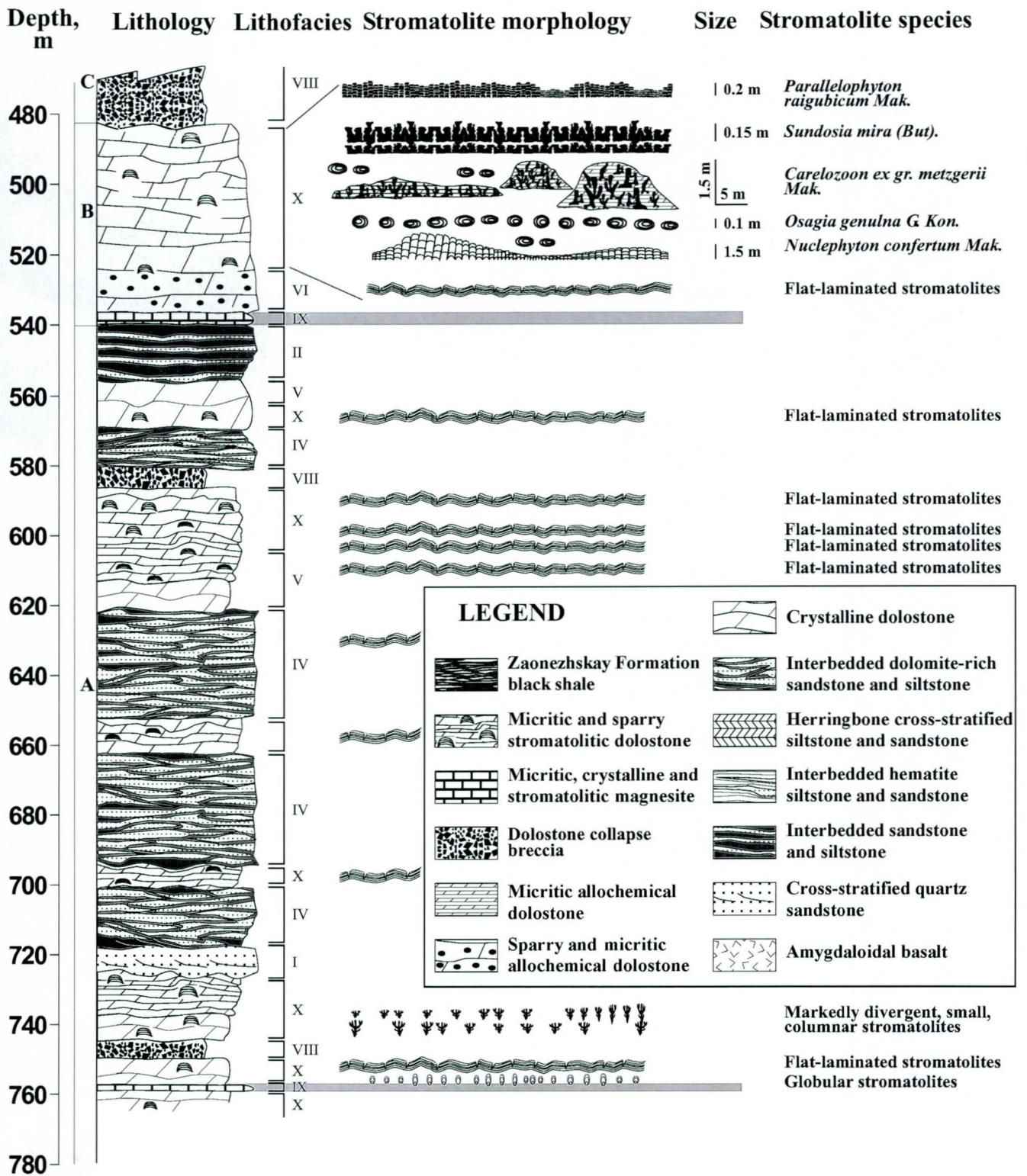
Figure 3.   The main stromatolite morphologies versus lithostratigraphy, drillhole 4699.
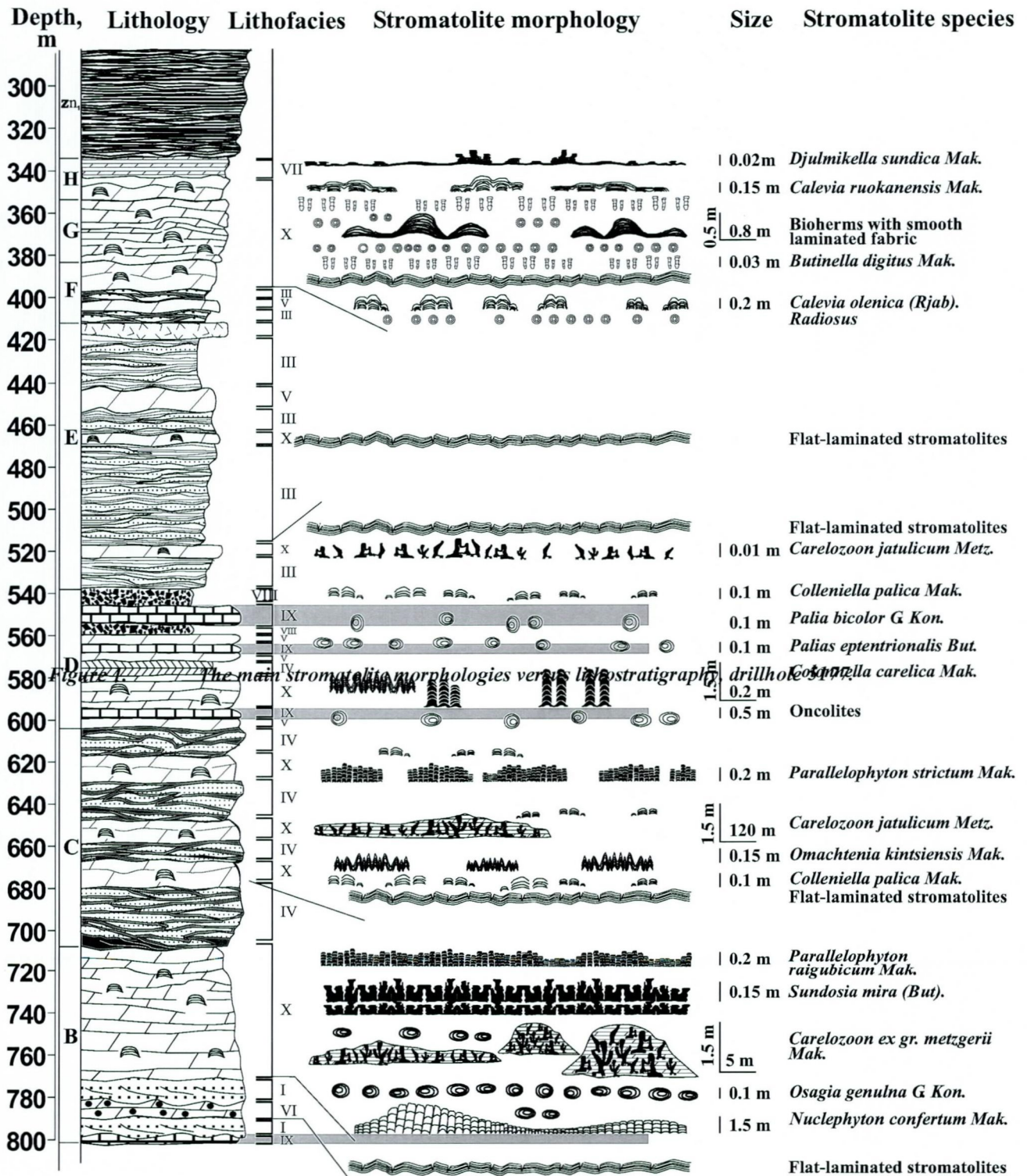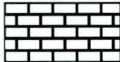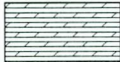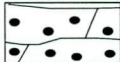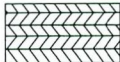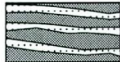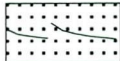
Figure 4. *The main stromatolite morphologies versus lithostratigraphy, drillhole 5177.*

LEGEND

(hatched pattern)	Zaonezhskay Formation black shale
(pattern)	Micritic and sparry stromatolitic dolostone
(brick pattern)	Micritic, crystalline and stromatolitic magnesite
(breccia pattern)	Dolomite collapse breccia
(lined pattern)	Micritic allochemical dolostone
(dotted pattern)	Sparry and micritic allochemical dolostone
(wavy pattern)	Crystalline dolostone
(pattern)	Interbedded dolomite-rich sandstone and siltstone
(chevron pattern)	Herringbone cross-stratified siltstone and sandstone
(lined pattern)	Interbedded hematite siltstone and sandstone
(dark lined pattern)	Interbedded sandstone and siltstone
(dotted pattern)	Cross-stratified quartz sandstone
(v pattern)	Amygdaloidal basalt

Legend for Figures 3 & 4.

Lithofacies II is a 20 m-thick unit of sandstones interbedded with siltstones in the uppermost part of Member A. The sedimentary rocks are either thin-bedded or lenticular-bedded, the latter being expressed by the development of sandstone layers in silty beds. An apparent lack of tidal reworking leaves the beds intact. The sedimentological features are consistent with an occasionally flooded supratidal zone on a tidal flat.

Lithofacies III is recognised by intercalated brown, hematite siltstones and pink quartz sandstones which are only developed in Member E. Sandstones are the dominant lithology. They are mature, platy, cross-stratified and characterised by carbonate cement. The sandstones form 5 to 70 cm-thick layers and in places contain quartz-hematite pebbles. The siltstones are dark grey, mud-cracked and hematite-rich. The fine laminae of the siltstones characteristically define low-relief hummocks and swells with amplitudes of less than 1 cm and wavelengths of 1-3 cm. A 1 to 2 m-thick bed of clastic hematite ore and halite cube casts in siltstones has been reported from this lithofacies (Akhmedov et al. 1993). A 50 m-thick flow of amygdaloidal basalt has been observed to be locally developed in the uppermost part of the Lithofacies III. The presence of halite pseudomorphs and absence of calcium sulphate evaporites is

15

perhaps consistent with a non-marine origin (Southgate 1986) for Lithofacies III. Given the widespread development of desiccation cracks and small-wavelength wave ripples, either a playa lake environment or a ponded tidal flat setting under evaporitic conditions may be proposed. The amygdaloidal structure of the basalt suggests volcanic eruption in a subaerial environment.

Lithofacies IV consists of grey, beige and pale pink, fine-grained, dolomite-rich sandstones and siltstones. Many of the layers show distinctive herringbone cross-bedding, flaser bedding and tidal bedding. The latter is composed of regular cycles of silt and sand, or cross-bedded sand layers and lenses between silty material. Lithofacies IV has been recognised in Members A, C, D and F. Most of the field characteristics may be assigned to a lower energy, tidal and supratidal sandflat.

Lithofacies V is composed of white, grey, beige or pink, crystalline dolostones. In most cases, beds of crystalline dolostones are typically structureless or indistinctly parallel-laminated. Shaly laminae are very common. Their discontinuity suggests an origin by pressure solution. Micritic dolostones and marls of Members B, C and D are sporadically marked by desiccation cracks (Fig. 5a) and by dolomite pseudomorphs after small crystals of gypsum (Akhmedov et al. 1993). The latter are distinguished by the 'swallow tail' twin morphology typical of gypsum developed under subaqueous conditions. Syndepositional deformation expressed as tepee structures is a common feature of Member C (Akhmedov et al. 1993). The overall field observations match chemical precipitation of carbonate in a low-energy setting, e.g., upper tidal zones of protected bights and/or lagoons. However, the significance of the tepee structures is not yet clear. In general, tepee structures can develop in both a submarine environment and at, or near, a subaerially exposed surface. A modern environment of arid or semi-arid climate along a coastal plain is considered to be most favourable for the development of massive tepees, as evidenced by modern Australian coastal plain environments where tepees are reported from surface crust (e.g. Handford et al. 1984). There are at least two important settings for the development of extensive tepee zones in ancient carbonate deposits. The Precambrian (e.g., Rocknest) and Permian (e.g. Carlsbad) examples are associated with a shallow peritidal or island environment (an exposed barrier) located at the seaward margin of carbonate platforms (e.g. Demicco & Hardie 1994). The Triassic examples signify subaerial exposure of the carbonate

(a)

(b)

(e)

(c)

(d)

17

Figure 5. *Photographs of drillcore illustrating sedimentological features of rocks of the Tulomozerskaya Formation. (a) Bedding surface between two pale pink dolostone layers extending from upper left to lower right corner. The bedding surface is marked by desiccation cracks filled with sandy material (pale grey). Drillhole 5177, depth 604.0 m. The lowermost part of Member D, Lithofacies V, upper tidal zone of protected lagoon. (b) Red, structureless dolorudite. Intraclasts are oolitic dolostones (white and grey) and red, hematite-rich, sparry and micritic dolostones (red). Drillhole 4699, depth 535.5 m. The lower part of Member B, Lithofacies VI, low-energy protected bight. (c) Red breccia of stromatolitic dolostones related to a tepee structure. Note marginal reddening of some of the fragments (lower right corner) which suggests that the breccia was exposed to air and subjected to oxidation. Drillhole 5177, depth 670.0 m. Member C, Lithofacies X, upper tidal zone of carbonate flat. (d) Red, flat-laminated, weakly domed stromatolites with fenestrae (blister stromatolite). Stromatolite laminae are cracked and syngenetically brecciated which resulted in the development of a clotted fabric. Drillhole 5177, depth 660.0 m. Member C, Lithofacies X, drained depressions and ephemeral ponds in an upper tidal carbonate flat. (e) Red, finely laminated siltstone. Note light-coloured bleaching zones and 'roll structure' developed along more permeable sandstone layers. Bleaching is due to the introduction of reducing solutions to the red siltstone. Solutions were likely derived from overlying C_{org}-rich sediments of the Zaonezhskaya Formation during late diagenesis-catagenesis. The beds are transitional from the Tulomozerskaya to the Zaonezhskaya Formation, lacustrine environment.*
Core diameter in all cases is 42 mm.

platform for extended periods due to lower amplitude sea-level low stands (Hardie et al. 1986; Goldhammer at al. 1990).

Lithofacies VI is a grainstone. Advanced recrystallisation hampers a distinction between laminated, intact layers of dolostones and grainstones. Although dolostones from a few layers are dolarenite and dolorudite (Figs. 3 & 4), the limited development of grainstones may be an artefact caused by a high degree of recrystallisation which obliterated the primary structure of the carbonates. Dolarenite and dolorudite are very characteristic features of Member B, though they have also been observed in Member A. Members F and H only occasionally contain layers of dolostones which are considered as dolarenite and dolorudite. In most cases, beds of grainstone are red, typically structureless (Fig. 5b) or crudely stratified by variations in colour and grain

size. Shaly laminae are very common. Sparry allochemical dolostones predominate, whereas micritic varieties have a very limited development. Allochem size ranges from 0.1 (dolarenite) to 8 mm (dolorudite). Allochems are represented by unsorted and angular intraclasts of micritic, oolitic and sparry dolomite. Other clasts are rounded quartz grains and sporadic hematite and siliceous oolites. Cement, when preserved, is represented by a syntaxial dolomite spar overgrowth on micritic, oolitic and sparry dolomite intraclasts (Fig. 6). These overgrowths are cloudy and rich in inclusion. Generally, burial syntaxial overgrowths are clear whereas inclusion-rich
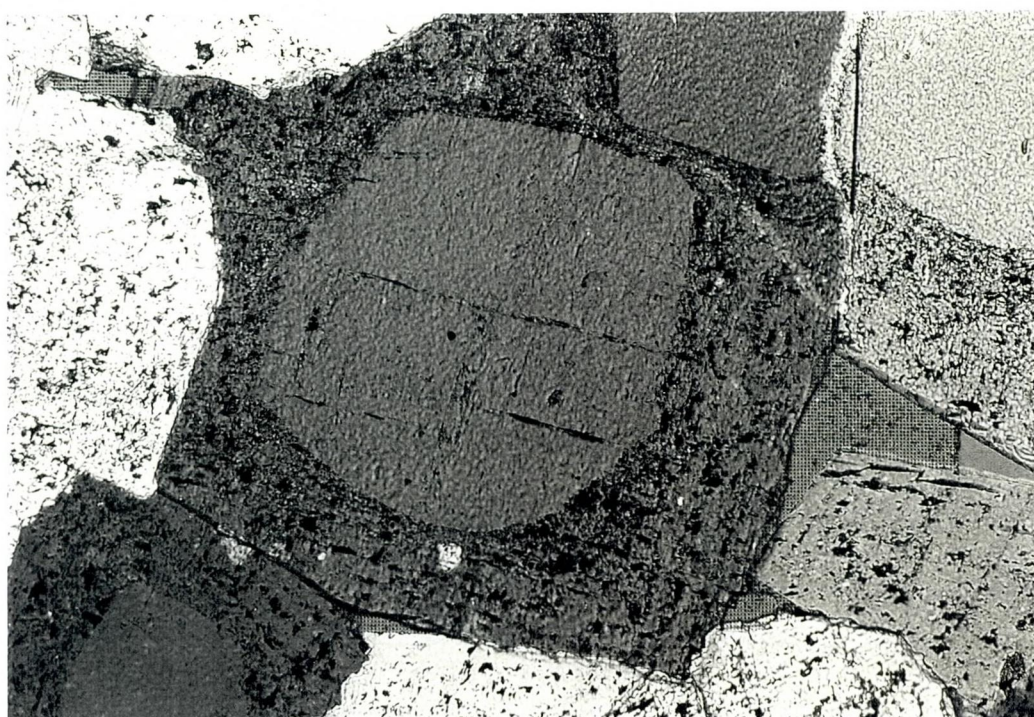
Figure 6.   *Syntaxial dolomite spar overgrowth on a dolomite clast (recrystallised oolite ?).*
                Member B dolarenite. Cross-polarised light. Drillhole 4699, depth 506.0 m. Long
                axis of photomicrograph is 1.2 mm.

and cloudy, syntaxial, dolomite spar is considered to represent earlier overgrowths (e.g. Tucker & Wright 1990, pp. 351-352). Clear, syntaxial, dolomite overgrowths, which apparently precipitated in the burial environment, have been documented only once. The matrix of sparry allochemical dolostones may be classified as either

crystalline dolomite (Fig. 7a) or, to a lesser extent, mosaic dolomite spar. In both cases dolomite is rich in gas/fluid inclusions (Fig. 7b). The latter may indicate that the matrix has undergone diagenetic alteration at low water/rock ratios (e.g. Carpenter & Lohman 1997). Abundant vugs, voids (filled with drusy dolomite) and cauliflower-like aggregates of quartz with crude radial fabric (Fig. 8a) are very characteristic features. The cauliflower-quartz contains plentiful gas/fluid-filled inclusions or empty micropores (Fig. 8b). The shape of individual crystals of quartz resembles those of gypsum. On this basis, these aggregates are considered here as pseudomorphs after sulphates. Sedimentological characteristics of Lithofacies VI indicate a depositional environment in a relatively low-energy setting, apparently developed in protected bights.

Lithofacies VII comprises red or brown, fine-grained, thinly laminated, micritic, allochemical dolarenites which are entirely developed in the uppermost part of Member H. Allochems are represented exclusively by dolomitic oolites. Dolostones contain relics of primary porosity (i.e. birdseyes) and vugs filled with cryptocrystalline quartz suggesting that the sediments were frequently exposed to the oxygenated air. These sedimentological features point to a lower-energy supratidal setting.

Lithofacies VIII is represented by collapse dolostone breccias, which occur in the lower and upper parts of Member A, at the base of Member C, and in the upper part of Member D. In all cases, breccias appear as poorly cemented fragments of brown, pink and white dolostones embedded in insoluble residues (namely, dark brown dolomite-sericite-chlorite material enriched in iron oxide). As no palaeokarst surfaces have been observed, the sub-surface dissolution of evaporite mineral phases is considered to have been the main process leading to the development of collapse breccias. Although a palaeoenvironmental interpretation of Lithofacies VIII is hampered by limited field observations on the lateral extension of the layers containing collapse breccias, we suggest a playa lake or sabkha setting to be the most likely environmen.

Lithofacies IX is represented by magnesites and magnesite-rich dolostones. All the magnesites and magnesite-bearing dolostones form 3 to 15 m-thick beds in Members A, B and D. Magnesites are white, grey, yellowish, fine- to coarse-grained,

(a)
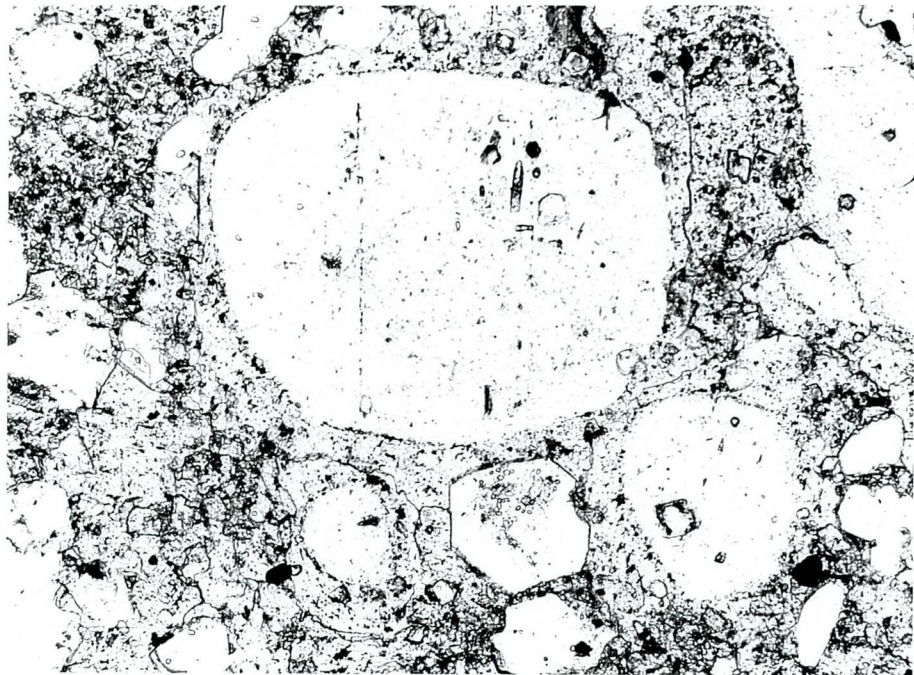
(b)
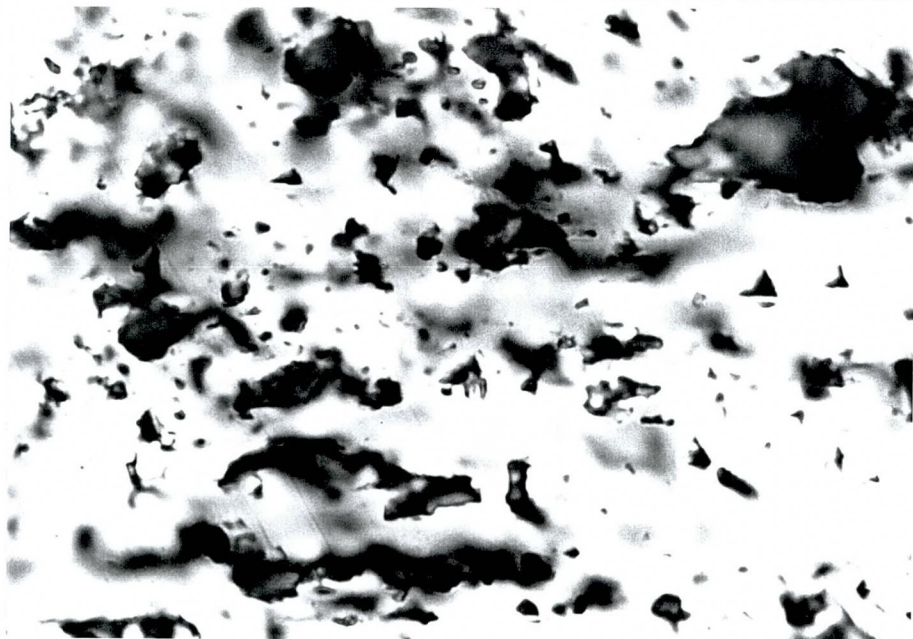
Figure 7.   *(a) Photomicrograph of dolarenite from Member B. The dolarenite is composed of recrystallised oolites and dolostone clasts in a 'dusty', sparry dolomite matrix. Plane-polarised light. Drillhole 4699, depth 522.5 m. Long axis of photomicrograph is 1.2 mm. (b) Gas/fluid inclusions in dolomite spar, matrix of Member F dolarenite. Plane-polarised light. Drillhole 5177, depth 392.7 m. Long axis of photomicrograph is 0.1 mm.*
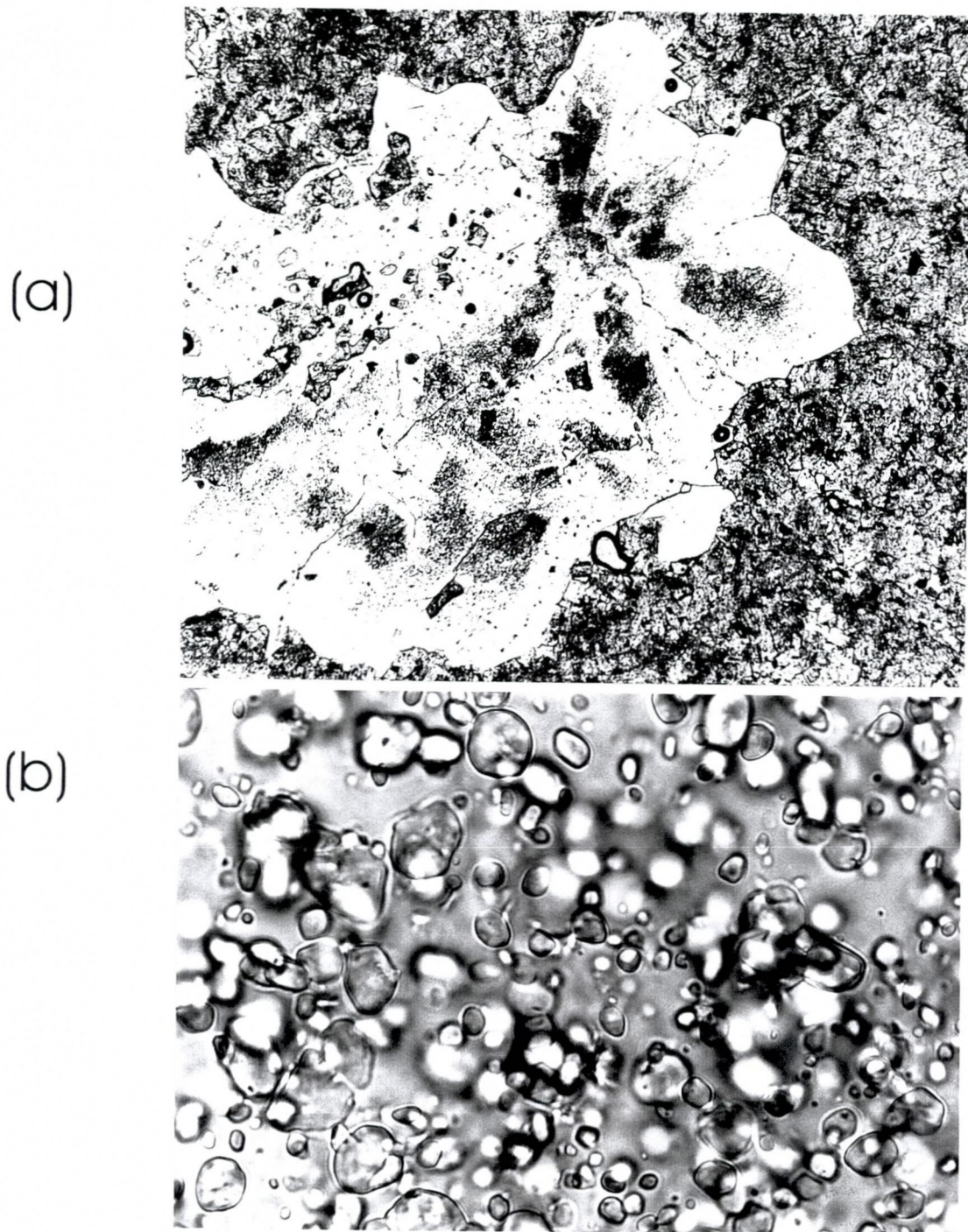
Figure 8.   (a) Photomicrograph of quartz aggregate with crude radiating structure. Member B
sparry allochemical dolostone. Quartz with cloudy appearance due to the presence
of gas/fluid inclusions. Plane-polarised light. Drillhole 4699, depth 524.1 m. Long
axis of photomicrograph is 3.0 mm. (b) Gas/fluid inclusions in radiating aggregate
of quartz. Member B sparry allochemical dolostone. Plane-polarised light.
Drillhole 4699, depth 535.5 m. Long axis of photomicrograph is 0.1 mm.

structureless rocks. The magnesite lithofacies has been discussed in detail by Melezhik et al. (submitted). They have assigned magnesite to sabkha (similar to sabkha magnesites of Abu Dhabi) and playa (similar to the Coorong Lagoon district and Lake Walyungup coastal playa magnesites, Australia) environments.

Lithofacies X is a stromatolitic mat lithofacies. It is represented by microbial laminae, which form persistent beds of variable thickness, columnar stromatolites and a variety of biostromal and biohermal stromatolites. Columnar stromatolites and oncolites are very abundant in Members B, C, D and G. In other members, stromatolites and oncolites are only occasionally developed. In some places stromatolitic beds are deformed into tepee structures (Akhmedov et al. 1993). Breccias of stromatolitic dolostones related to the tepee structure have been observed in Member F (Fig. 5c). Flat-laminated stromatolitic layers of Members A and E have always been observed to be multicoloured, highly cracked and syngenetically brecciated (Fig. 5d).

In most cases the stromatolitic dolostones have undergone recrystallisation. When fine lamination is preserved, the thin, dark laminae are predominantly dolomicrite and the thicker, light laminae are dolospar. In general, the boundaries between the laminae are not sharp.

The palaeoenvironmental interpretation of the stromatolitic lithofacies is presented in the following sections.

5.   RED BEDS

Red coloration is an essential feature of the rocks of the Tulomozerskaya Formation, particulary of those developed in Members A, B, C, E, G and H. These rocks, together with the Lower Jatulian sequence, have been described in the literature as a classic example of Palaeoproterozoic 'red beds' (e.g. Sochava 1979). The designation 'red beds' may sound inconsistent with the presence of abundant stromatolites developed throughout the sequence. Highly abundant and diverse stromatolites indicate that the

Onega palaeobasin was characterised by very intensive microbial activity, which should have resulted in a high bioproduction and accumulation of organic material. Because of this, one might consider the red colour to be the result of post-depositional transformation of the rocks, e.g., oxidation or migration of organic material with the superimposed introduction of oxidising fluids (Kaufman, personal communication 1998). In fact, there are several lines of evidence that the red colour is a primary phenomenon, caused by the presence of terrigenous particles of hematite. In many cases, hematite enriches the steeper slopes of ripple marks as well as the bottom sets of cross-stratified beds (Sokolov et al. 1970). Fragments from breccia in some of the tepee structures also show reddening, indicating that tepees were exposed to air (Fig. 5c). Both micritic and sparry dolomite contain hematite 'dust'. Many of the stromatolites display red coloration (Fig. 9), which we interpret to be a result of iron oxidation through photosynthetic activity of cyanobacterial mats. Additionally, rocks subjected to post-depositional (catagenetic) alteration are represented by bleaching and discoloration of the red beds. Bleaching occurs due to removal of oxidised iron by reducing solutions migrating within permeable layers ('roll structures', Fig. 5e). To conclude, we believe that the intact 'red beds' of the Tulomozerskay Formation indicate the presence of free oxygen in both the atmosphere and the basinal water. Why and how the accumulated organic material has been removed from stromatolites is a subject that will be discussed elsewhere.

6.   BIOFACIES

In general, stromatolite-forming algae interact in a complex way with environmental conditions, both at microscopic and macroscopic levels (Cohen et al. 1977; Krumbein et al. 1977). As no reliable microfossils have been detected in the drillcores investigated, our biofacies is limited to macroscopic study, namely stromatolite morphologies. Strictly speaking, stromatolites are organosedimentary structures produced by sediment trapping, binding and/or the precipitation activity of micro-organisms, primarily by cyanobacteria (e.g. Walter 1976).
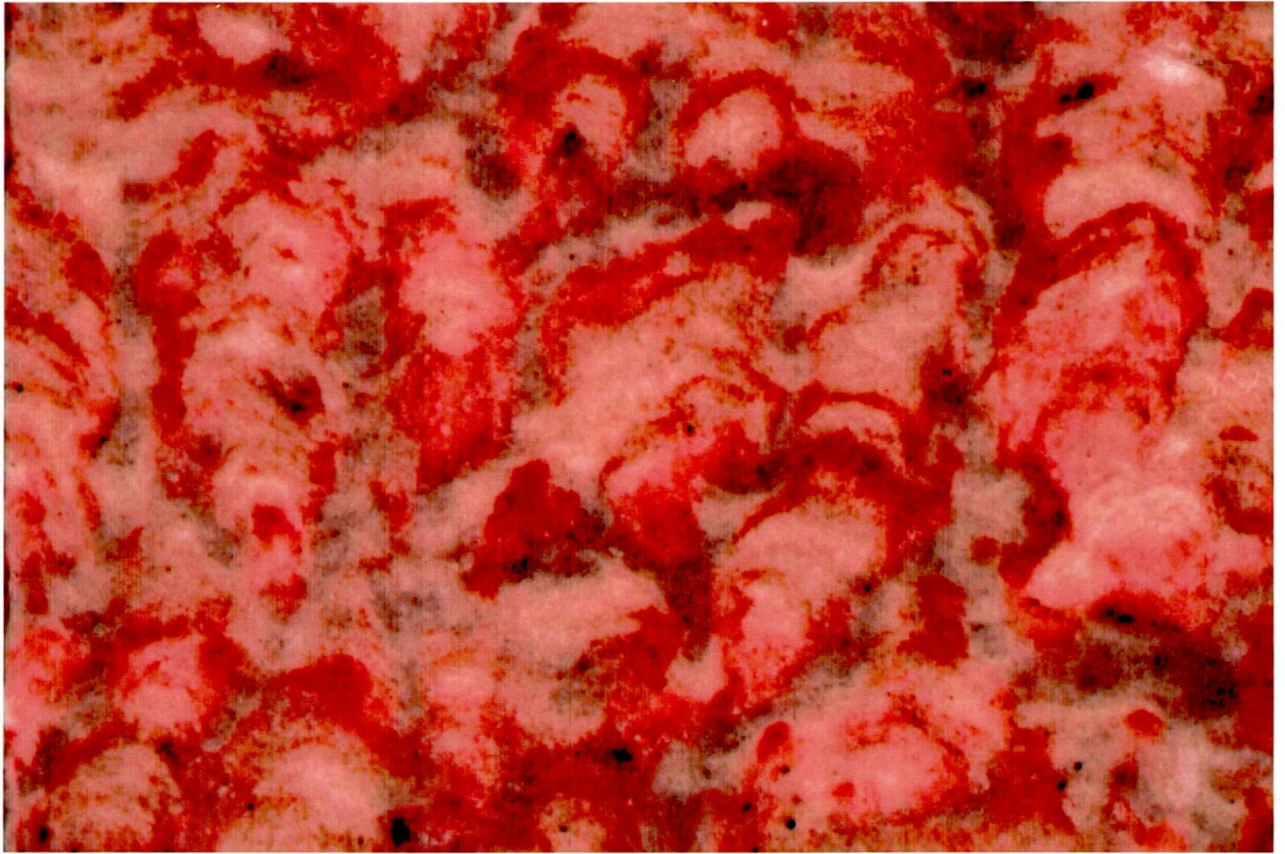
Figure 9.　　　　*Red, columnar stromatolites from Member C. Note intercolumnar space filled with light grey and white dolarenite whereas the stromatolite laminae and the margins of column are composed of pink dolomite. The pink colour is interpreted to have formed due to photosynthetically induced precipitation of iron oxide in an extremely shallow-water environment.*

Biostromal and biohermal stromatolites of the Tulomozerskaya Formation come in a diverse array of sizes and shapes (Makarikhin & Kononova 1983). Figs. 3 and 4 summarise the distribution of the principal stromatolite morphologies versus stratigraphy. Some of these stromatolite developments have been found in the drillholes studied, though the majority have been described from outcrops near the drilling sites. The stromatolite morphologies may be grouped into the following types:

(1) Flat-laminated stromatolites forming lower relief sheets are a characteristic feature of Members A and E. They have also been documented in the lower part of Member B and in the middle parts of Members C and F. In most cases, laminated stromatolites developed on a carbonate substrate (Fig. 10a). Laminae shapes vary

from wrinkled on the 1–2 mm scale, to weakly domed on the 3–5 mm scale (blister stromatolite mat). Layers of laminated stromatolites are very commonly cracked and appear as either an indistinct, clotted fabric (Fig. 5d, 10b) or a ribbon fabric with polygonal prism cracks. Common developments are inorganic laminations with algal partings. Desiccation cracks developed on surfaces of the flat-laminated stromatolites apparently led to the nucleation and formation of globular stromatolites with indistinct boundaries, which occupy the space within individual polygons (Fig. 10c). The majority of laminated stromatolites exhibit fenestrae filled with a later generation of euhedral dolomite crystals. Carbonate material composing wrinkled and weakly domed stromatolite laminae has a red colour and is enriched in hematite.

(2) Laterally continuous biostromes are the most abundant type showing the development of columnar stromatolites. Stromatolites are characterised by smooth, simple convex laminations. The thickest (2-3 m) developments of biostromes have been documented in the middle part of Member B where they are composed of markedly divergent columns of red *Sundosia mira (But)*. Another type of markedly divergent columnar stromatolites, red *Carelozoon jatulicum Metz.*, composes thick (up to 2 m) biostromes in the middle part of Member C. Biostromes of *Nuclephyton confertum Mak.* (branching columnar stromatolites) are composed of tightly packed columns. The columns are larger in the middle parts of bioherms, become smaller – fining towards the margins – and have a sharp contact with surrounding intraclastic dolostones (Fig. 10d). Laminae of stromatolites consist of red, hematite-rich dolomite. A series of biostromes in the upper parts of Members B and C consists of tightly packed, elongated columns of *Parallelophyton raigubicum Mak.* and *Nuclephyton confertum Mak.* (Fig. 10e), respectively. They have gently arched upper surfaces with a ridged morphology (Fig. 11a). *Omachtenia kintsiensis Mak.* and branching columns of *Djulmekella sundica Mak.* form thin biostromes in Members C and H, respectively.

(3) Very close-spaced bioherms with convex-up domes 0.8 m wide and very gently dipping margins, are separated by either pale grey, laminated, fine-grained dolostones or red, hematite-rich, structureless, dolorudites containing oncolites *Radiousus* sp. This type of bioherm is found in the uppermost part of Member G.

26

(a)

(b)

(c)

(d) →

(e)

Figure 10.   *Photographs of drillcore and outcrops illustrating sedimentological features of the Tulomozerskaya Formation stromatolites. (a) Structureless dolarenites (light brown, lower half of drill core) serve as substrate for weakly domed stromatolites which are, in turn, overlain by flat-laminated stromatolites. Member G. Drillhole 5177, depth 360.0 m. (b) Pink, weakly domed and flat-laminated stromatolites are cracked and separated by dolarenite with the development of an indistinct, clotted fabric. Member B. Drillhole 4699, depth 520.4 m. (c) Bedding surface of flat-laminated stromatolites with polygonal desiccation cracks. Note globular stromatolite with indistinct boundaries developed within individual polygons (lower left corner). Member B. Southwestern shore of Sundozero Lake. (d) Bedding surface of biostrome (columnar Nuclephyton confertum Mak.) in sharp contact with crudely bedded dolarenite. Note smaller columns developed along the biostrome margin. Member B. Southwestern shore of Sundozero Lake. (e) Elongated columns of Nuclephyton confertum Mak, bedding surface. Member B. Southwestern shore of Sundozero Lake. Core diameter is 42 mm, length of knife 24 cm.*

(4) Spaced bioherms are most abundant in the middle of Member B (Fig. 4). Bioherms are surrounded by red, hematite-rich, structureless, dolostones; one type being composed of *Karelozoon metzgerii Mak.* (markedly divergent, branching columnar stromatolites). These bioherms are cupola-like buildups 3-5 m wide and 1.5 m high with steeply dipping margins (Fig. 11b). However, the relief of the stromatolite domes above the surrounding sediment surface (synoptic relief) is difficult to determine. Based on sporadically observed single laminae enveloping the full height of the bioherm, one may suggest that the synoptic relief was at least 20 cm.

(5) Spaced, single, large columns of *Colonnella carelica Mak.* are 0.2 m wide and up to 1.5 m high. Columns are either tightly packed or largely separated by grey laminated dolostones (Fig. 12) and are composed of grey and pale grey, diffuse laminae consisting of dolomite enriched (up to 30%) in clastic quartz. This type of stromatolite morphology is rather rare and a typical feature of the lower part of the Member D dolostones.

(6) Oncolites have been documented throughout the sequence, although they are most typical for Member G and for layers associated with magnesite (Fig. 3-4).
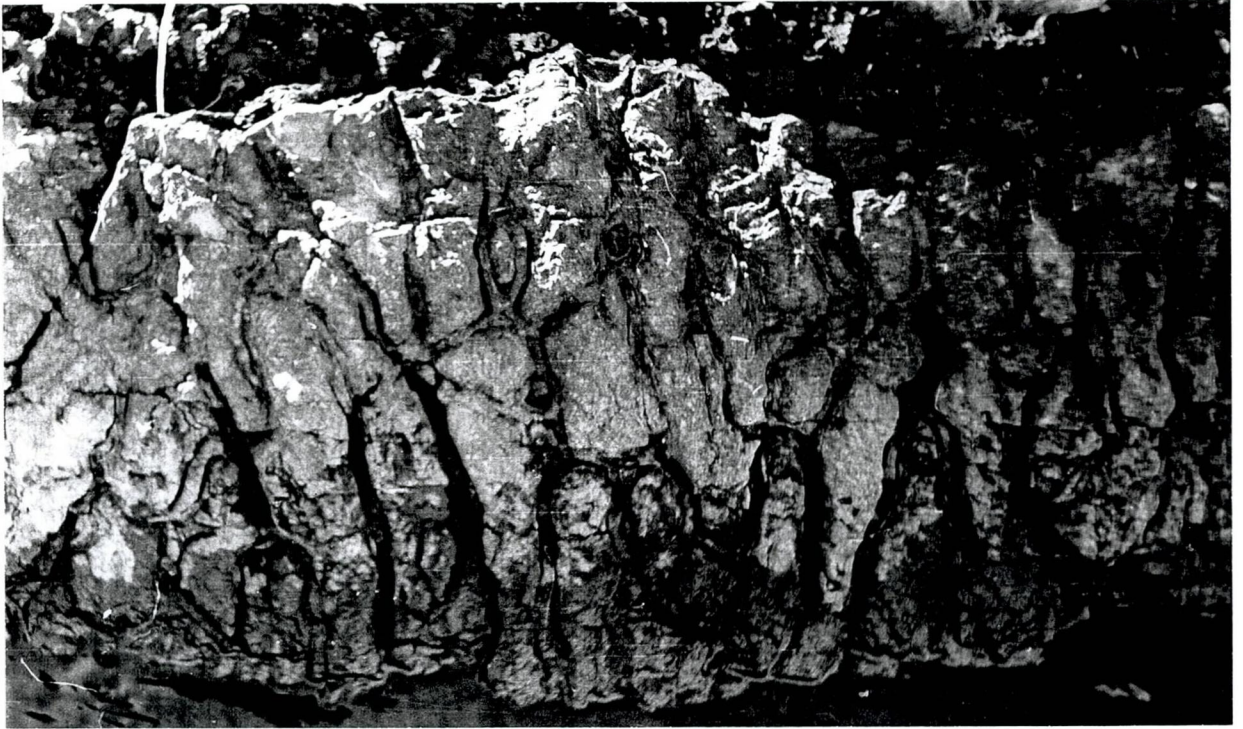
Figure 11.   *Stromatolite morphologies. (a) Parallelophyton raigubicum Mak. Ridge structure on the surface of biostrome. Member B. Length of outcrop is 125 cm. (b) Cupola-like bioherm composed of Carelozoon metzgerii Mak. Southwestern shore of Sundozero Lake near Raiguba. Member B. Length of hammer is 70 cm. Both photographs are reproduced from Makarikhin & Kononova (1983).*

29

7. PALAEOENVIRONMENTAL INTERPRETATION OF STROMATOLITE MORPHOLOGIES

It has been shown (for references see Golubic, 1976) that the specifically different environmental requirements of cyanobacteria have resulted in their distribution and dominance being dependent on environmental conditions and constraints. Within these constraints, environmental factors may additionally affect stromatolite morphology. As shown by the example of Shark Bay (e.g., Hoffman, 1976; Playford & Cockbain, 1976), discrete columnar forms (0.4 m high) occur on headlands fully exposed to waves, and have been found in tidal and intertidal environments. The relief of the columns is proportional to the intensity of wave action. Elongated columns, with elongation developed parallel to the direction of wave attack, form in less exposed bights near headlands. Ridge and rill structures with reliefs of 0.1-0.3 m occur in areas partially protected from wave attack. Small embayments completely protected from waves are represented by stratiform sheets with lower relief.

Based on the criteria outlined above one can posit that the lower relief, flat-laminated stromatolite sheets of the Tulomozerskaya Formation might have formed in an environment where wave and tidal scour was weak. This may have developed throughout an intertidal zone of protected embayments, as well as in protected embayments and protected parts of an upper intertidal zone in bights (see Shark Bay stromatolites, Hoffman 1976). The presence of blister, clotted fabrics with fenestrae requires a lower supratidal zone (e.g. Hoffman 1976). However, the desiccation cracks commonly observed in the flat-laminated stromatolite sheets may suggest that they formed in drained depressions and ephemeral ponds in an upper tidal zone of a carbonate flat. This type of environment is assigned entirely to Member A (Fig. 3) and to the lowermost dolostones of Members B and C. The majority of flat-laminated stromatolite lithofacies of Member E probably formed in more evaporative conditions (e.g., playa lake environment) as they are interbedded with Lithofacies III containing halite casts.

Laterally continuous biostromes, mostly composed of small branching columnar stromatolites, are the next most abundant type of stromatolite lithofacies. In general,

30

Figure 12.   *Large column of Colonnella carelica Mak.sp.nov. Member D. West face of
Kintsiniemi quarry near Little Janisjarvi Lake. Length of hammer is 70 cm.
Photograph is reproduced from Makarikhin & Kononova (1983).*

31

this stromatolite morphology formed in intertidal environments. As the intertidal substrate is unstable, stromatolitic mats cannot colonise loose sand, and can initially only be established on lithified crusts in order to develop further discrete columns. The small diameter and low relief of branching columns in the Tulomozerskaya Formation place further constraints on the depositional environment. Such stromatolite morphologies are consistent with intertidal settings in protected bights, as is again evident from the Shark Bay example (Hoffman 1976). This assignment is also supported by the development of small-scale ridged structures, which are typical features of Members B and C Parallelophyton.

Spaced bioherms, very close-spaced bioherms, as well as spaced, large, and in places solitary columns are rare in the Tulomozerskaya Formation. They have been found in the middle parts of Members B, C and the lowermost portion of Member C. Spaced columns and spaced bioherms, particular those of Member G, are associated with abundant oncolites (Fig. 4). As discrete columnar structures occur where wave and tidal scour are strong, and their relief is proportional to wave action (Hoffman, 1976), we suggest that these particular stromatolites of the Tulomozerskaya Formation indicate intertidal settings close to shorelines fully exposed to wave action. Alternatively, they might have formed in sub-tidal settings. For example, in modern environments large (up to 2 m high), solitary stromatolites are known from actively migrating areas of Bahamian ooid shoals (e.g., Dill et al., 1986). Abundant oncolites favour both assumptions (e.g. Tucker & Wright 1990, p. 10).

8.   CONCLUSIONS (DEPOSITIONAL PALAEOENVIRONMENTS)

The Palaeoproterozoic Tulomozerskaya Formation that we have studied represents a 800 m-thick magnesite-stromatolite-dolomite-'red beds' sequence formed in a variety of environmental settings, including a complex combination of shallow-marine and non-marine conditions, as summarised in Table 1.

Terrigeneous red beds developed throughout the sequence and exhibit great variation in thicknesses and lithofacies. The lowermost quartzitic sandstones represent a meandering fluvial system over a carbonate coastal plain. Terrigeneous red beds, forming the middle part of the sequence, are consistent with a periodically flooded supratidal zone, ponded tidal flat and playa lake environment under high-temperature, evaporitic conditions.

A significant part of the carbonate rocks is stromatolitic, formed in peritidal shallow-marine settings. These carbonates display features of lower energy deposits accumulated in protected, partly closed environments such as bights or barred basins.

The flat-laminated stromatolitic dolostones of Members A and C may be assigned to a restricted evaporative environment developed in either ephemeral ponds in upper tidal zones, or coastal sabkhas and playa lakes. The red coloration of the carbonates indicates their frequent exposure to the air.

Only a small proportion of carbonates, developed in the middle part of Member B, at the base of Member D, and particularly in Member G, represent deposits which accumulated in relatively 'open' environments. They show some analogy to carbonates deposited in an environment exposed to strong wave action.

The abundant stromatolites developed in closed evaporitic or semiclosed environments of many lithofacies might have caused disequilibrium between atmospheric CO_2 and dissolved inorganic carbon in the local aquatic reservoir. This should be taken into account when interpreting the carbon isotope composition of the Tulomozerskaya carbonates. Careful discrimination is needed between local and global factors before the full interpretation of the carbon isotope excursion (and its implications) can be assessed.

ACKNOWLEDGEMENTS

REFERENCES

Akhmedov, A.M., Krupenik, V.A., Makarikhin, V.V. & Medvedev, P.V. 1993:
*Carbon isotope composition of carbonates in the early Proterozoic
sedimentary basins*. Printed report, Institute of Geology of the Karelian
Scientific Centre, Petrozavodsk, 58 pp. (in Russian).

Baker, A. J. & Fallick, A. E. 1989a: Evidence from Lewisian limestone for
isotopically heavy carbon in two-thousand-million-year-old sea water.
Nature **337**, 352-354.

Baker, A. J. & Fallick, A. E. 1989b: Heavy carbon in two-billion-year-old marbles
from Lofoten-Vesterålen, Norway: Implications for the Precambrian carbon
cycle. *Geochimica et Cosmochimica Acta* **53**, 1111-1115.

Carpenter, S.J. & Lohman, K.C. 1997: Carbon isotope ratios of Phanerozoic marine
cements: Re-evaluation the global carbon and sulphur systems. *Geochimica
et Cosmochimica Acta* **61**, 4831-4846.

Cohen, Y., Krumbein, W.E., Goldberg, M. & Shilo, M. 1977: Solar Lake (Sinai). 1.
Physical and chemical limnology. *Limnology and Oceanography* **22**, 597-
608.

Demicco, R.V. & Hardie, L.A. 1994: *Sedimentary Structures and Early Diagenetic
Features of Shallow Marine Carbonate Deposits*. Society of Sedimentary
Geology, Tulsa, Oklahoma, U.S.A.

Dill, R.F., Shinn, E.A., Jones, A.T., Kelly, K. & Steinen, R.P. 1986: Giant subtidal
stromatolites forming in normal salinity water. *Nature* **324**, 55-58.

Eskola, P. 1919: Hufvuddragen av Onega-Karelians geologi. Meddelanden från
Geologiska Föreningen I Heisingsfors år 1917 och 1919, 13.

Goldhammer, R.K., Dunn, P.A. & Hardie, L.A. 1990: Depositional cycles, composite
sea-level changes, cycle stacking patterns, and the hierarchy of stratigraphic
forcing: Examples from Alpine Triassic platform carbonates. *Geological
Society of America Bulletin* **102**, 535-562.

Golubic, S. 1976: Organisms that build stromatolite. *In*: Walter, M.R. (ed.)
Stromatolites. Elsevier Scientific Publishing Company, Amsterdam, Oxford,
New York, 113-126.

Hardie, L.A., Bosellini, A. & Goldhammer, R.K. 1986: Repeated subaerial exposure
of subtidal carbonate platforms, Triassic, northern Italy: evidence for high
frequency sea level oscillations on a 104 year scale. *Paleoceanography* **1**,
447-457.

Hoffman, P. 1976: Environmental diversity of Middle Precambrian stromatolites. *In*:
Walter, M.R. (ed.) *Stromatolites*. Elsevier Scientific Publishing Company,
Amsterdam, Oxford, New York, 599-611.

ISSC (International Subcommision on Stratigraphic Classification of IUGS
Commission on Stratigraphy). 1976. *In*: Hedberg, H.D. (ed.) *International
Stratigraphic Guide: A Guide to Stratigraphic Classification, Terminology
and Procedure*. John Willey & Sons, New York, 1-200.

Karhu, J. A. 1993: Palaeoproterozoic evolution of the carbon isotope ratios of
sedimentary carbonates in the Fennoscandian Shield. *Geological Survey of
Finland Bulletin* **371**, 1-87.

Karhu, J.A. & Holland, H.D. 1996. Carbon isotopes and rise of atmospheric oxygen.
Geology **24**, 867-879.

Kratz, K.O. 1963: Geology of the Karelian Karelides. *Transactions of the Laboratory
of Precambrian Geology of the USSR Academy of Sciences* **16**, 1-205. (in
Russian).

Krumbein, W.E., Cohen, Y. & Shilo, M. 1977: Solar Lake (Sinai). 4. Stromatolitic cyanobacterial mats. *Limnology and Oceanography* **22**, 635-656.

Makarikhin, V. V. & Kononova, G. M. 1983: *Early Proterozoic Phytolithes of Karelia.* Nauka, Leningrad. (in Russian).

Melezhik, V.A. & Fallick, A.E. 1996: A widespread positive $\delta^{13}C_{carb}$ anomaly at around 2.33-2.06 Ga on the Fennoscandian Shield: a paradox? *Terra Nova* **8**, 141-157.

Melezhik, V.A. & Fallick, A.E. 1997: Paradox regained? Reply. *Terra Nova* **9**, 148-151.

Melezhik, V.A., Fallick, A.E., Medvedev, P.V. & Makarikhin, V.V. Palaeoproterozoic magnesite: lithological and isotopic evidence for playa/sabkha environments. *Sedimentology* (submitted).

Negrutza, V. Z. 1984: *Early Proterozoic Development of the Eastern Part of the Baltic Shield.* Nedra, Leningrad. (in Russian).

Playford, P.E. & Cockbain, A.E. 1976: Modern algal stromatolites at Hamelin Pool, a hypersaline barred basin in Shark Bay. *In*: Walter, M.R. (ed.) *Stromatolites.* Elsevier Scientific Publishing Company, Amsterdam, Oxford, New York, 389-411.

Pukhtel', I.S., Zhuravlev, D.Z., Ashikhmina, N.A., Kulikov, V.S. & Kulikova V.V. 1992: Sm-Nd age of the Suisarskay suite on the Baltic Shield. *Transactions of the Russian Academy of Sciences* **326**, 706-711. (in Russian).

Schidlowski, M., Eichmann, R. & Junge, C.E. 1976: Carbon isotope geochemistry of the Precambrian Lomagundi carbonate province, Rhodesia. *Geochimica et Cosmochimica Acta* **40**, 449-455.

Sederholm, J.J. 1899: Über eine archaishe Sediment Formation in sudwestlichen
        Finland and ihre Bedeutung fur die Erklarung der Enstehungweise des
        Grundgebirges. *Bulletin de la Commission Géologique de Finlande* **6**, 254.

Sochava, A.V. 1979: *Precambrian and Phanerozoic 'Red Beds'.* , Nauka, Leningrad.
        (in Russian).

Sokolov, V.A. 1970: *Jatuli of Karelia and vicinities.* DSc Thesis, Geological Institute
        of the USSR Academy of Sciences, Moscow. (in Russian).

Sokolov, V.A. 1980: Jatulian formations of the Karelian ASSR. *In:* Silvennoinen, A.
        (ed.) *Jatulian Geology in the Eastern Part of the Baltic Shield,* Proceedings
        of a Finnish-Soviet Symposium held in Finland, 21th-26th August, 1979.
        Rovaniemi. The Committee for Scientific and Technical Cooperation
        between Finland and Soviet Union, pp. 163-220.

Sokolov, V.A. 1987: The Jatulian Superhorizon. *In:* Sokolov, V.A. (ed.) *The Geology
        of Karelia.* Nauka, Leningrad. (in Russian).

Sokolov, V.A., Galdobina, L.P.,Ryleev, A.B., Catzuk, Yu.I. & Kheskanen, K.I. 1970:
        Geology, sedimentology and palaeogeography of the Jatuli, Central Karelia.
        Institute of Geology, Karelian Science Centre, Petrozavodsk, Russia. (in
        Russian).

Southgate, P.N. 1986: Depositional environment and mechanism of preservation of
        microfossils, upper Proterozoic Bitter Springs Formation, Australia. *Geology*
        14, 683-686.

Tucker, M.E. & Wright, V.P. 1990: *Carbonate sedimentology.* Oxford.

Väyrynen, H. 1933: Über die Stratigraphie der Karelischen Formationen. *Bulletin de
        la Commission Géologique de Finlande* **101**, 54-78.

Walter, M.R. (ed.) 1976: *Stromatolites*. Elsevier Scientific Publishing Company, Amsterdam, Oxford, New York.

Yudovich, Ya.E., Makarikhin, V.V., Medvedev, P.V. & Sukhanov, N.V. 1991: Carbon isotope anomalies in carbonates of the Karelian Complex. *Geochemica International* **28(2)**, 56-62.